

PAPER • OPEN ACCESS

Influence of angular mismatch between pre- and post-irradiation scans for optical-CT gel readout: simulation based study

To cite this article: Yi Du *et al* 2019 *J. Phys.: Conf. Ser.* **1305** 012021

View the [article online](#) for updates and enhancements.



IOP | ebooks™

Bringing you innovative digital publishing with leading voices to create your essential collection of books in STEM research.

Start exploring the collection - download the first chapter of every title for free.

Influence of angular mismatch between pre- and post-irradiation scans for optical-CT gel readout: simulation based study

Yi Du^{1,2,3}, Xiangang Wang^{2*}, Xincheng Xiang², Hao Wu^{1**} and Yves De Deene

¹Key laboratory of Carcinogenesis and Translational Research (Ministry of Education/Beijing), Department of Radiotherapy, Peking University Cancer Hospital & Institute, 52 Fucheng Road, Beijing, 100142, China

²Institute of Nuclear & New Energy Technology, Tsinghua University, Beijing, 100084, China

³School of Engineering, Faculty of Science and Engineering, Macquarie University, Sydney, NSW 2109, Australia

E-mail: *wangxiangang@tsinghua.edu.cn; **13552661030@139.com

Abstract. The pre- and post-irradiation scan strategy for optical-CT gel readout often turns out to be corrupted by angular mismatch between these two scans. In this study, we used computational simulations to investigate the influence of angular mismatch. Two phantoms are constructed: one cylindrical phantom with synthetic impurities and one elliptical phantom. The reconstructed results of angular mismatched pre- and post- data show that the dual-scan method is very sensitive to repositioning error, and *positive-negative pair errors* can be easily identified around impurities and phantom edges. From the simulation results, we believe that the angular mismatch should be less than 0.1 degree.

1. Introduction

Since the gel dosimeter was first proposed by Gore in 1984 [1], optical-CT has become a major readout modality for gel-based 3D radiotherapy dose distribution measurement, utilizing the property of quantitative optical density changes (ΔOD) induced by localized absorbed dose [2]. Several system designs have been proposed over the past decades [3, 4] and two compact scanners are now commercially available (VistaTM by Modus Medical Devices Inc., and OCTOPUSTM by MGS Research Inc.). Despite variations in system design, all optical-CT scanners utilize the common physical principle [5]: tomographic OD maps of gel dosimeters are reconstructed from traverse projection data captured at each angle over 360 degrees, and then absolute dose maps can be derived by calibration of ΔOD to dose.

An ideal gel dosimeter is expected to be homogeneous. However, in the process of fabrication and measurement, gel dosimeter phantoms often appear to be *imperfect* with impurities, such as dust or air bubbles inside gel matrix, stains or scratches on phantom surfaces, and seams of phantom holders, all of which degrade signal quality and reconstructed OD maps by noise and artifacts. In order to improve image quality and only obtain ΔOD maps in gel dosimeters, the strategy of using pre- scan and post-irradiation scans is commonly used [6-8]. However, although phantoms are repositioned very carefully for post scan, all too often resultant ΔOD maps turn out corrupted by phantom imperfections, which



nevertheless leads us to question the reproducibility of the pre- and post- scan method. In this study, we used computational simulations to investigate the influence of angular mismatch between pre- and post-irradiation scans and discussed the required accuracy for phantom repositioning.

2. Methods and materials

2.1. Synthetic Phantoms

In this study, two synthetic phantoms were designed with ΔOD maps to mimic dose distributions irradiated by a 6-MV Linac with 100-cm SSD.

2.1.1. Cylindrical Phantom with Impurities. Since most gel dosimeters are prepared in cylindrical holders, a cylindrical phantom similar to the one in [9] was used, which was 10-cm in height and 10-cm in diameter shown in Figure 1(a). The irradiation field was 2-cm \times 2-cm and 2-cm offset from the central axis(CAX). It is noted that, to investigate the behaviour of phantom imperfections in angular mismatch, a pair of two-pixel patches along the z-direction on the phantom surface were constructed to simulate holder seams; in the meantime, two bright seven-pixel particles were constructed to simulate strains: one in the irradiation field and the other in the gel matrix.

2.1.2. Elliptical Phantom. With the advent of non-water dosimeters (Presage [10, 11] and FlexyDos3D [12, 13]), dosimeters can be mechanically strong enough to be cast in anthropomorphic shapes. To study the influence of angular mismatch to non-cylindrical phantoms, an elliptical phantom was built as shown in Figure 1(c), which was 10-cm in height 10-cm in major-axis and 5-cm in minor axis. The irradiation field was 1-cm \times 1-cm and 2-cm off CAX along x-direction.

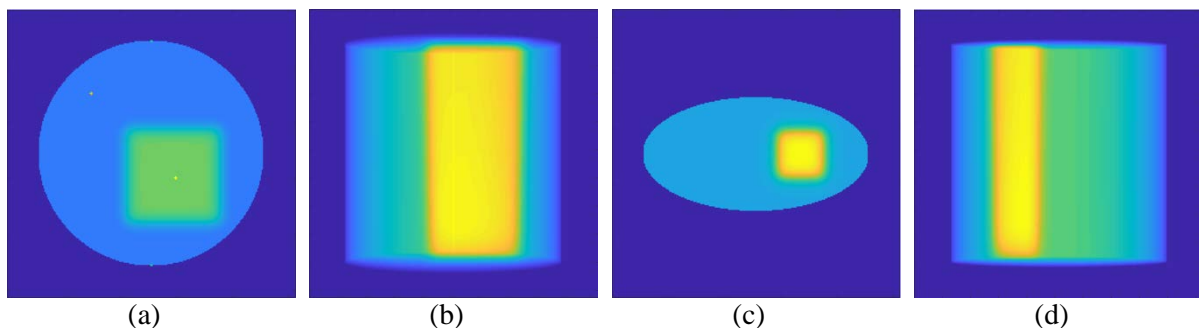


Figure 1. Defected cylindrical phantom: (a) central axial slice and (b) projection image; Elliptical phantom: (c) central axial slice and (d) projection image.

2.2. Modelling of Optical-CT Imaging and Angular Mismatch

We used the specifications of our Vista optical-CT scanner for geometry definition. 360 logarithmic projections from 0-degree to 359-degree of 1-degree interval were generated using the GPU accelerated pixel-driven algorithm [14]. To model the dual-scan method, the synthetic phantoms without ΔOD patches were first utilized to generate projections as pre-irradiation logarithmic data (*Ref*); then the phantoms with ΔOD s were used to generate post-irradiation logarithmic data (*Data*), as shown in Figure 1(b)&(d).

To model the angular mismatch between *Ref* and *Data*, during *Data* generation we shifted all the projection angles by a small constant value (δ), which means *Ref* and *Data* are angularly mismatched by δ . Three mismatch scenarios were performed for both phantoms with $\delta = 0.1, 0.5$ and 1.0 degree respectively. The projections by subtracting *Ref* from *Data* were used for tomographic image reconstruction using FDK (Hann filter) algorithm [15].

3. Results & Discussion

3.1. Cylindrical Phantom with Impurities

The reconstructed images with zoomed details on the synthetic impurities are given in Figure 2, along with difference maps between the $\delta = 0$ image. From the difference maps, we can see that when pre- and post- data are not perfectly matched, the impact of phantom impurities can be easily identified. What's worse, the impurities impair image quality by forming *positive-negative pulse pairs* in the reconstructed images, and as δ increases pulse pairs become obvious.

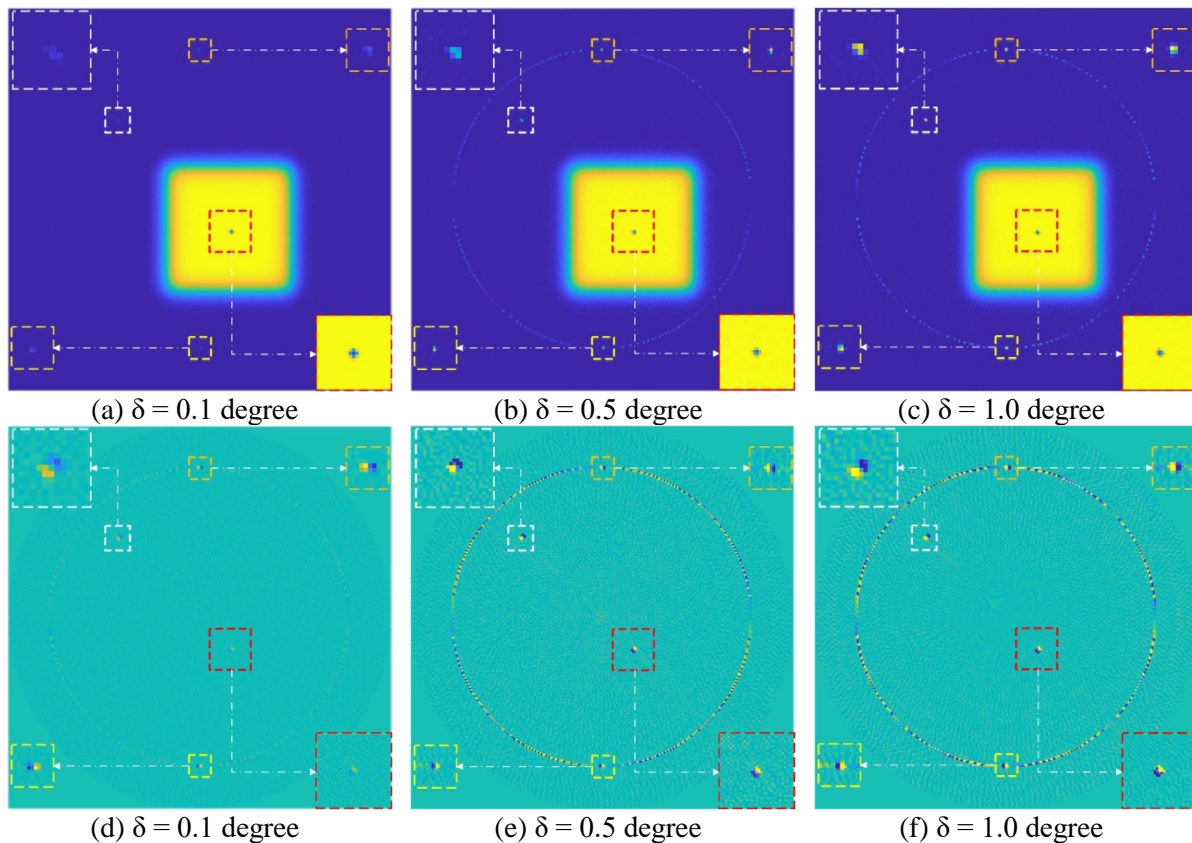


Figure 2. Reconstructed images with zoomed details when the angles are mismatched by (a) 0.1 degree, (b) 0.5 degree and (c) 1.0 deg. Difference maps with zoomed details between the perfect matching resultant image and (a) (b) and (c) are shown in (d) (e) and (f) respectively.

3.2. Elliptical Phantom

The reconstructed images of the elliptical phantom are given in Figure 2, with difference maps between $\delta = 0$ image as well. Since the traverse distance over the phantom at each angle is not the same, we can see that the angular mismatch leads to a *positive-negative ring errors* around the phantom edge, and the ring becomes thicker as δ increases.

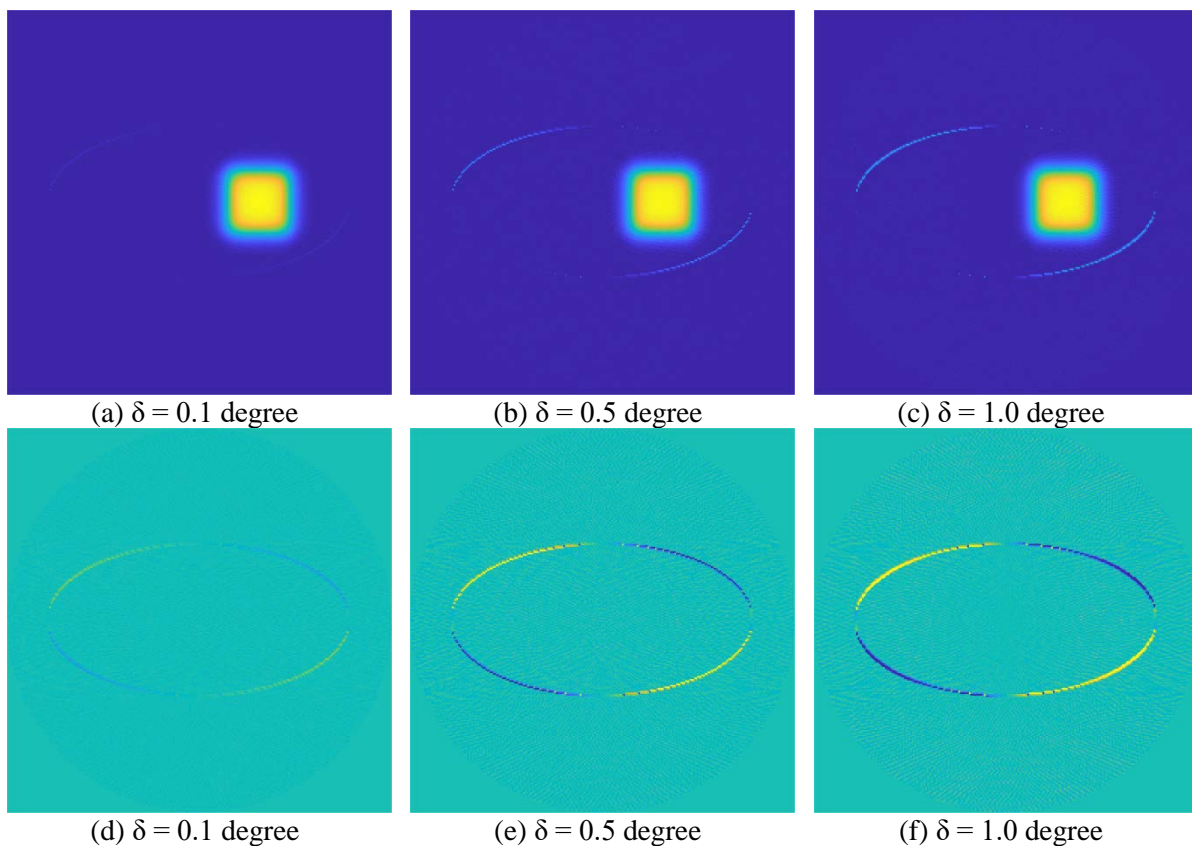


Figure 3. Reconstructed images with zoomed details when the angles are mismatched by (a) 0.1 degree, (b) 0.5 degree and (c) 1.0 degree. Difference maps with zoomed details between the perfect matching resultant image and (a) (b) and (c) are shown in (d) (e) and (f) respectively.

4. Conclusions

In this study, we can see that the pre- and post-irradiation scan method for optical-CT gel readout is very sensitive to repositioning error, and even when angular mismatch is as small as 0.1 degree, *positive-negative pair errors* can be identified around impurities and phantom edges. It is noted that the processes of scattering, reflection and refraction are not taken into account in the simulation, which all deflect light direction during light propagation. As a result, the influence of angular mismatch would be much more complicated in real cases, which implies that to obtain proper image quality the angular matching accuracy between pre- and post- scan data should be less than 0.1 degree. Considering the accuracy requirement, rather than using a precisely designed mechanical registration stage, we believe algorithm-based data registration or image processing would be a feasible cost-effective choice.

5. Acknowledgement

Jointly Supported by Beijing Natural Science Foundation (No. 1184014, 1174016), National Science Foundation of China (No. 61571262, 11575095), China Postdoctoral Science Foundation (No. 2017M620542) and National Key Research and Development Program (No. 2016YFC0105406).

6. References

- [1] Gore J C and Kang Y S 1984 *Phys. Med. Biol.* **29** 1189-97
- [2] Baldock C 2009 *J. Phys.: Conf. Ser.* **164** 012002
- [3] Baldock C et al 2010 *Phys. Med. Biol.* **55** R1-63
- [4] Doran S J 2009 *J. Phys.: Conf. Ser.* **164** 012020

- [5] Jordan K J 2017 *J. Phys.: Conf. Ser.* **847** 012019
- [6] Wu C-S and Xu Y 2010 *J. Phys.: Conf. Ser.* **250** 012044
- [7] Doran S J 2013 *J. Phys.: Conf. Ser.* **444** 012004
- [8] Doran S J 2010 *J. Phys.: Conf. Ser.* **250** 012086
- [9] Du Y *et al* 2017 *J. Phys.: Conf. Ser.* **847** 012069
- [10] Schreiner L J 2015 *J. Phys. Conf. Ser.* **573** 012003
- [11] Khezerloo D *et al* 2017 *Radiat. Phys. Chem.* **141** 88-97
- [12] De Deene Y *et al* 2015 *Phys. Med. Biol.* **60** 1543-63
- [13] Høye E M *et al* 2015 *J. Phys.: Conf. Ser.* **573** 012067
- [14] Du Y *et al* 2017 *Biomed. Eng. Online* **16** 2
- [15] De Deene Y 2015 *J. Phys.: Conf. Ser.* **573** 012076